Quadrupole-mediated dielectric response and the charge-asymmetric solvation of ions in water

Stephen J. Cox,[1] Kranthi K. Mandadapu,[2,3] and Phillip L. Geissler[2,4]
[1)] *Yusuf Hamied Department of Chemistry, University of Cambridge, Lensfield Road, Cambridge CB2 1EW, United Kingdom*[a)]
[2)] *Chemical Sciences Division, Lawrence Berkeley National Laboratory, Berkeley, CA 94720, United States.*
[3)] *Department of Chemical Engineering, University of California, Berkeley, CA 94720, United States.*[b)]
[4)] *Department of Chemistry, University of California, Berkeley, CA 94720, United States.*[c)]

(Dated: 24 March 2021)

Treating water as a linearly responding dielectric continuum on molecular length scales allows very simple estimates of solvation structure and thermodynamics for charged and polar solutes. While this approach can successfully account for basic length and energy scales of ion solvation, computer simulations indicate not only its quantitative inaccuracies but also its inability to capture some basic and important aspects of microscopic polarization response. Here we consider one such shortcoming, a failure to distinguish the solvation thermodynamics of cations from that of otherwise-identical anions, and we pursue a simple, physically inspired modification of the dielectric continuum model to address it. The adaptation is motivated by analyzing the orientational response of an isolated water molecule whose dipole is rigidly constrained. Its free energy suggests a Hamiltonian for polarization fluctuations that accounts implicitly for the influence of higher-order multipole moments, while respecting constraints of molecular geometry. We propose a field theory with the suggested form, whose nonlinear response breaks the charge symmetry of ion solvation. An approximate variational solution of this theory, with a single adjustable parameter, yields solvation free energies that agree closely with simulation results over a considerable range of solute size and charge.

I. INTRODUCTION

Water is perhaps the most important solvent, and understanding the fundamental physical principles that underlie aqueous solvation is essential to a broad range of disciplines, such as protein structure and dynamics, desalination, atmospheric chemistry and crystallization. Despite numerous studies over the past century, major gaps in our understanding of aqueous solvation still exist, particularly for small, charged solutes and for environments that are spatially heterogeneous. Highlighting these gaps, active research continues to develop and apply increasingly sophisticated methods of spectroscopy[1–6] and computer simulation[7–15] in order to clarify the solvation of ions in aqueous systems.

These limits on our understanding are reflected by the lack of a robust, general, and thoroughly predictive theory for the microscopic structure and thermodynamics of water's response to charged solutes. As a promising and historically significant starting point, dielectric continuum theory (DCT) – a macroscopic linear response theory for solvent polarization – can be applied in a microscopic context. This approach has yielded insights that imbue modern perspectives on solvation, but its flaws and limitations are considerable. Among the most straightforward and important microscopic applications of DCT, the Born model of solvation[16] caricatures an ionic solute as a volume-excluding, uniformly charged sphere of radius R embedded in a continuous, linearly-responding solvent medium with dielectric constant ϵ. Reversibly introducing the solute's charge q in this model gives a change in free energy

$$F_{\rm chg}^{\rm (Born)}(q) = -\frac{q^2}{2R}\left(\frac{\epsilon-1}{\epsilon}\right) \tag{1}$$

that explains the basic energy scale of ion solvation and its sensitivity to solute size and charge, and asserts the permittivity as an essential determinant of solvent quality. Its quantitative predictions are roughly correct, provided that the dielectric radius R is treated as an empirical parameter similar but not identical to the radius R_0 of molecular volume exclusion.

Fig. 1 shows the Born estimate of the charging free energy $F_{\rm chg}(q)$, alongside results of molecular simulation of the SPC/E model of water,[17] as a function of solute charge for several solute sizes R_0. Relative to $F_{\rm chg}(e)$, where e is the charge of an electron, agreement is reasonable even for ions as small as fluoride. But absolute errors of $\sim 50 k_{\rm B}T$ (where T is the temperature and $k_{\rm B}$ is Boltzmann's constant) overwhelm the scale of typical thermal fluctuations. Despite the magnitude of these errors, DCT continues to serve as a basis for quantifying the thermodynamics of aqueous response in calculations that cannot afford to represent water molecules explicitly.[18] Motivated in part by such usage, this paper describes theoretical efforts to improve on DCT while maintaining the simplicity underlying its appeal.

[a)] Electronic mail: sjc236@cam.ac.uk
[b)] Electronic mail: kranthi@berkeley.edu
[c)] Electronic mail: geissler@berkeley.edu

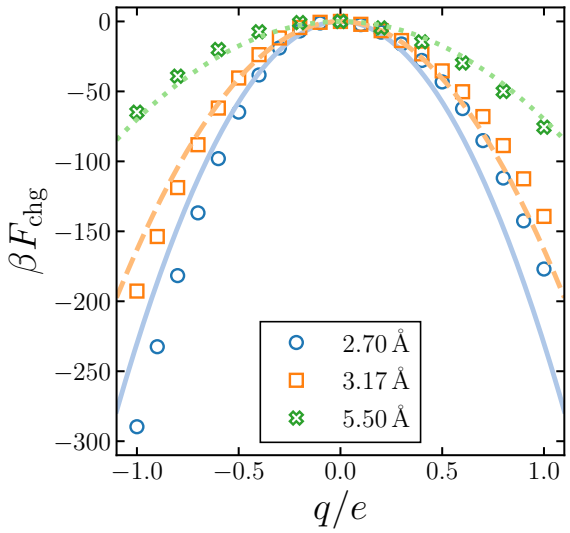

FIG. 1. Solute charging free energy $F_{\rm chg}$ vs q for different solute sizes R_0, as indicated in the legend. Symbols show results from simulations, while lines show best-fits of $F_{\rm chg}^{\rm (Born)}(q)$ (Eq. 1) to $F_{\rm chg}$. $F_{\rm chg}^{\rm (Born)}(q)$ largely captures the overall scale and size dependence of $F_{\rm chg}$, but it does not describe the asymmetric solvation[19–21] of anions vs cations.

From a molecular perspective, DCT is remarkably undetailed, resolving neither the tetrahedral motifs defining water's hydrogen bond network nor the features of molecular geometry that are responsible for it. Significant improvement might well require an approach that differs substantially in both spirit and methodology. Indeed, there is ample evidence that near-field contributions from a solute's immediate environment have a different character than contributions from more distant molecules. The idea that the latter are well described by DCT, while the former are not, has figured prominently in many theoretical and computational approaches to describing aqueous environments. The inner-shell of Marcus theory,[22] for example, acknowledges and empirically addresses such a distinction in the nature of near-field and far-field response. More directly relevant to our study, the multi-state Gaussian model[23] of single ion solvation similarly presumes that local solvent-structure requires special treatment, while far-field response obeys simple Gaussian statistics. A precise and systematic computational framework for range separation in solvation can be found in the quasi-chemical theory (QCT)[7,24,25] developed by Pratt and co-workers. These hybrid theories and methodologies can achieve a high degree of accuracy, e.g. when QCT is used in combination with *ab initio* treatment of electronic structure.[26,27] But they are not nearly as flexible or generalizable as DCT.

In the next section we describe in detail the specific and fundamental shortcoming of DCT that inspires our theoretical development, namely, an inability to distinguish between the solvation of cations and anions that differ only in the sign of their charge. The contrastingly strong charge asymmetry observed in molecular simulations is then framed in terms of a water molecule's higher-order multipole moments, with particular emphasis on the molecular quadrupole. Sec. III shows, in the context of a single water molecule, how integrating out quadrupole fluctuations renormalizes statistics of the molecular dipole. The result of that molecular calculation is then used to motivate a generalized version of DCT, whose predictions for ion solvation thermodynamics are approximately explored and numerically evaluated in Sec. IV. We end with a discussion and outlook in Sec. V.

II. BACKGROUND THEORY AND SIMULATION

A. Charge asymmetric solvation

This paper focuses on one key failing of DCT, evident in Fig. 1 for the solvation of ions in bulk liquid water. Specifically, in molecular simulations cations and anions of the same size can have very different solubilities, while DCT in its simplest form lacks such charge asymmetry completely. Interfacial solvation provides even more striking examples of charge asymmetry, with some anions adsorbing favorably to the liquid's outermost layer while their cationic counterparts are strongly depleted. Here we will consider only the bulk case.

The lack of charge aymmetry in DCT can be readily appreciated from its basic mathematical structure. As a linear response theory, DCT in its simplest form can be cast as a microscopic model for a Gaussian fluctuating polarization field $\mathbf{m_r}$, with energy[28]

$$\mathcal{H}_{\rm dip}[\mathbf{m_r}] = \frac{1}{2}\sum_{\mathbf{r}}\sum_{\mathbf{r}'}\mathbf{m_r}\cdot\left[\left(\frac{4\pi}{\epsilon-1}\right)v^{-1}\,\mathbf{I}\,\delta(\mathbf{r}-\mathbf{r}') + \nabla\nabla'\frac{1}{|\mathbf{r}-\mathbf{r}'|}\right]\cdot\mathbf{m}_{\mathbf{r}'} \tag{2}$$

where $\mathbf{I}$ is the identity tensor. This model can be equivalently formulated in continuous space,[29] but it will later become more convenient for us to view space discretely. We therefore take the position vector $\mathbf{r}$ to index a lattice cell with microscopic volume v and $\mathbf{m_r}$ to be a coarse-grained representation of the molecular dipole distribution within v. The coarse-graining transformation could take many forms, and we will not specify one here. In-

troducing a solute with charge q, which we place at the origin without loss of generality, adds an electrostatic interaction between $\mathbf{m_r}$ and the solute's electric field $\mathbf{E}_q(\mathbf{r}) = -q\nabla r^{-1}$,

$$\mathcal{H}_{\mathrm{DCT}}[\mathbf{m_r}] = \mathcal{H}_{\mathrm{dip}}[\mathbf{m_r}] - \sum_{\mathbf{r}} \mathbf{E}_q(\mathbf{r}) \cdot \mathbf{m_r} \qquad (3)$$

Volume exclusion is acknowledged in this description only by restricting the sums in Eqs. 2 and 3 to lattice cells that are not occupied by the solute, a restriction we will leave implicit. The thermodynamic consequences of evacuating the solute's volume, while significant in some cases, are not considered by DCT and will not be accounted for here. Our focus on comparing cations and anions of the same size justifies this neglect, but is not meant to minimize the complex and interesting coupling between density and polarization fields, which is particularly important near interfaces.[30–33]

The field theoretic Hamiltonian in Eq. 3 is *charge symmetric*: Changing the sign of q, while simultaneously inverting the dipole field's orientation, leaves $\mathcal{H}$ invariant. Cation and anion solvation are thus statistically equivalent at this level of theory. The polarization field induced by a cation, under inversion, is identical to that induced by an anion of the same size. Predicted solubilities of the two ions are equal as a result, as is clear from the Born energy $F_{\mathrm{chg}}^{(\mathrm{Born})}(q)$ (Eq. 1) as an even function of q. By contrast, computer simulations indicate that ion solvation in water is significantly charge *asymmetric*. In their seminal study of single ion solvation using molecular simulation, Hummer *et al.*[34] clarified this charge asymmetry by presenting the average electrostatic potential $\langle V\rangle_q$ at the center of a volume-excluding solute as a function of q. For reference, we recapitulate those results in Fig. 2a for a solute with $R_0 = 3.17\,\text{Å}$ immersed in SPC/E water. Notably, this potential is negative even in the case of a neutral solute, $q = 0$, giving an impression that liquid water is intrinsically more hospitable to cations than to anions. The physical origins of this neutral cavity potential[9,20,21] $\langle V\rangle_0$ are surprisingly challenging to identify precisely; profound ambiguities plague any attempt just to separate contributions of solvent molecules near the solute and those of a distant interface.[13–15,35–40] Putting aside the lack of a clear physical interpretation, the effects of a nonzero neutral cavity potential are straightforward to include in the DCT framework. Adding an interaction between the solute and this innate potential,

$$\mathcal{H}_{\mathrm{DCT}}[\mathbf{m_r}; \langle V\rangle_0] = \mathcal{H}_{\mathrm{dip}}[\mathbf{m_r}] - \sum_{\mathbf{r}} \mathbf{E}_q(\mathbf{r}) \cdot \mathbf{m_r} + q\langle V\rangle_0, \qquad (4)$$

gives a simply modified solvation energy

$$F_{\mathrm{chg}}^{(\mathrm{Born})}(q; \langle V\rangle_0) = -\frac{q^2}{2R}\left(\frac{\epsilon - 1}{\epsilon}\right) + q\langle V\rangle_0. \qquad (5)$$

Modifying DCT in this simple way has little impact, however, on the predicted charging free energy, at least on the scale shown in Fig. 1. Furthermore, simulation results for fully charged ions indicate charge asymmetry in the direction opposite to $\langle V\rangle_0$, favoring solvation of anions over cations. Any significant improvements obtained by including the neutral cavity potential are limited to small values of q,[20,21] as shown in the Supporting Information (SI).

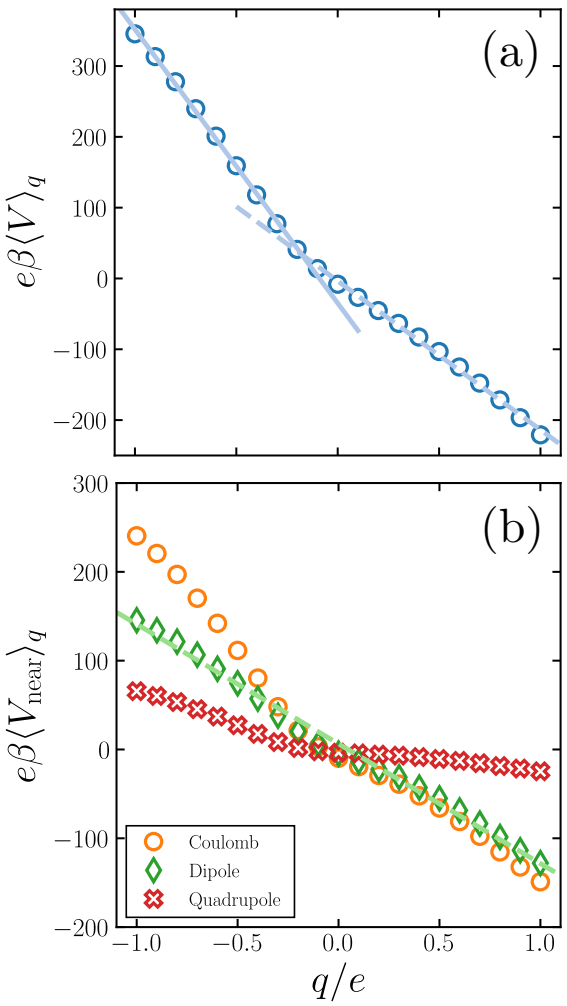

FIG. 2. Average electrostatic potential at the center of a volume-excluding solute, with size $R_0 = 3.17\,\text{Å}$ and charge q, due to the surrounding solvent. (a) All solvent molecules in the simulation are included (see Sec. VI). The solid and dashed lines are guides to the eye, suggesting distinct susceptibilities for $q/e < -0.2$ and $q/e > -0.2$, respectively. (b) Average electrostatic potential at the center of the solute due to molecules in the first coordination shell (those molecules with oxygen atoms within 3.5 Å of the solute's center). Along with the full Coulomb potential, the dipolar and quadrupolar contributions are also shown. The dashed green line is a guide to the eye, suggesting that the dipolar response in approximately linear. The quadrupolar response, by contrast, exhibits a 'kink' similar to that of the full Coulomb potential.

Deviations from charge symmetry in SPC/E water (and similar models) are not at all limited to an offset

in the solvent's electric potential. The polarization *response* to charging a solute is also distinct for cations and anions, with more substantial consequences.[15,20,21,34,41] Fig. 2a highlights this asymmetric response, which manifests in $\langle V\rangle_q$ as a nonlinear dependence on q. Amending DCT to account for this nonlinear response is much more challenging than introducing a background potential $\langle V\rangle_0$. Distinct thermodynamics for charging cations and anions can be engineered by using different dielectric radii in the Born model, as Latimer, Pitzer, and Slansky pursued with quantitative success.[19] More nuanced empirical approaches have been based on the approximately piecewise-linear character of $\langle V\rangle_q$, in essence asserting different values of ϵ in different ranges of q.[21] These *ad hoc* descriptions of ion solvation, however, fall short of the flexible field theory we are seeking. Such a theory would instead feature a microscopic Hamiltonian that is anharmonic in the dipole field $\mathbf{m}_\mathbf{r}$, generating distinct response to solute fields $\mathbf{E}_q$ with opposite signs of q as an emergent behavior. Below we will propose a theory of this form, motivated directly by the molecular fluctuations underlying polarization response.

B. Multipole expansion of the solvation potential

Charge asymmetric response in liquid water is rooted in the inequivalent distribution of positive and negative charge within each individual water molecule. A large molecular dipole is a characteristic feature of this distribution, but by itself it is a highly incomplete description. Electrostatic forces that underlie hydrogen bonding and charge asymmetry are instead encoded in higher order multipoles. Although a detailed description of these forces requires a multipole expansion to high order, we will argue that a low-order expansion may in fact be sufficient to correct qualitative flaws of DCT.

In order to isolate important sources of nonlinear polarization in computer simulations, we decompose the solvation potential $\langle V\rangle_q$ according to multipole moment and distance from the solute. Anticipating that deviations from linear response are dominated by the near-field environment, we show in Fig. 2b contributions to $\langle V\rangle_q$ from molecular dipoles and quadrupoles of water molecules in the solute's first solvation shell. The nonlinear shape of the total near-field contribution $\langle V_\mathrm{near}\rangle_q$ indeed strongly resembles the full potential $\langle V\rangle_q$. By contrast, contributions from more distant molecules, presented in the SI, depend linearly on q to a good approximation, confirming expectations from previous work that DCT accurately portrays polarization response on length scales beyond $\sim 1\,\mathrm{nm}$.[34,42–45]

The dipole contribution to $\langle V_\mathrm{near}\rangle_q$ for a solute at position $\mathbf{r}$ is defined as

$$\langle V^\mathrm{dip}_\mathrm{near}\rangle_q = -\Big\langle \sum_j h_{\mathrm{near},j}\boldsymbol{\mu}_j\cdot\nabla\frac{1}{|\mathbf{R}_j-\mathbf{r}|}\Big\rangle \qquad (6)$$

where

$$\boldsymbol{\mu}_j = \sum_\alpha q_\alpha \mathbf{r}_{j\alpha} \qquad (7)$$

is the net dipole of the j^th molecule, whose center resides at $\mathbf{R}_j$. $\mathbf{r}_{j\alpha}$ is the position of site α on molecule j, whose charge is q_α. The characteristic function $h_{\mathrm{near},j}$ is unity if the oxygen atom of solvent molecule j resides in the solute's first solvation shell; otherwise, it vanishes. Compared with $\langle V_\mathrm{near}\rangle_q$ and $\langle V\rangle_q$, the first-shell dipolar potential $\langle V^\mathrm{dip}_\mathrm{near}\rangle_q$ is a remarkably linear function of q. At large values of q, we expect significant nonlinearity in $\langle V^\mathrm{dip}_\mathrm{near}\rangle_q$ due to dielectric saturation, but for $|q|\le e$ such effects are barely apparent on the scale of Fig. 2.

By contrast, the quadrupolar contribution to $\langle V_\mathrm{near}\rangle_q$ exhibits a nonlinearity quite similar to that of the full potential. We define this contribution as

$$\langle V^\mathrm{quad}_\mathrm{near}\rangle_q = \frac{1}{2}\Big\langle \sum_j h_{\mathrm{near},j}\mathbf{K}_j : \nabla\nabla\frac{1}{|\mathbf{R}_j-\mathbf{r}|}\Big\rangle, \qquad (8)$$

where

$$\mathbf{K}_j = \sum_\alpha q_\alpha(\mathbf{r}_{j\alpha}-\mathbf{R}_j)(\mathbf{r}_{j\alpha}-\mathbf{R}_j) + (\mathrm{const})\mathbf{I} \qquad (9)$$

is the net quadrupole of the j^th molecule. The coefficient multiplying the identity tensor $\mathbf{I}$ in Eq. 9 is completely arbitrary, since $\mathbf{I}:\nabla\nabla|\mathbf{R}_j-\mathbf{r}|^{-1} = -4\pi\delta(\mathbf{R}_j-\mathbf{r})$ and $\mathbf{R}_j$ necessarily lies outside the solute. We will exploit this arbitrariness below, freely adding and removing isotropic contributions to $\mathbf{K}$ for convenience. Similar liberties can be taken with higher order multipoles.

Parsing $\langle V_\mathrm{near}\rangle_q$ as in Fig. 2b requires choosing the reference point $\mathbf{R}_j$ that sets the origin of a molecular coordinate system. The dipole $\boldsymbol{\mu}_j$ is not sensitive to this choice, but its contribution $\langle V^\mathrm{dip}_\mathrm{near}\rangle_q$ is. At higher orders, both the multipole moment (e.g., $\mathbf{K}_j$) and its contribution to the electric potential (e.g., $\langle V^\mathrm{quad}_\mathrm{near}\rangle_q$) depend on the choice of $\mathbf{R}_j$. For $\langle V^\mathrm{dip}_\mathrm{near}\rangle_q$ and $\langle V^\mathrm{quad}_\mathrm{near}\rangle_q$ we find only a weak sensitivity for reasonable choices of $\mathbf{R}_j$, i.e., points within the solute's excluded volume that lie along the line of symmetry bisecting the hydrogen atoms and running through the O atom. Throughout this work we will adopt the molecule's center of charge $\mathbf{R}^{(\mathrm{c})}_j \equiv \sum_\alpha |q_\alpha|\mathbf{r}_{j\alpha}/\sum_\alpha|q_\alpha|$, which is displaced $\sim 0.3\,\text{Å}$ from the O atom, as the reference point, which is shown schematically in Fig. 3a. Fig. 3b provides a visual argument for this choice of molecular reference frame. Isosurfaces are shown for the corresponding electric potential

$$\phi^{(2)}_j(\mathbf{r}) = -\boldsymbol{\mu}_j\cdot\nabla\frac{1}{|\mathbf{r}-\mathbf{R}_j|} + \frac{1}{2}\mathbf{K}_j:\nabla\nabla\frac{1}{|\mathbf{r}-\mathbf{R}_j|}, \qquad (10)$$

i.e., the multipole expansion of the potential generated by molecule j, truncated at second order. The strong resemblance to water's intramolecular geometry suggests that this low-order expansion captures aspects of charge

asymmetry essential to ion-specific solvation. By contrast, an analogous second-order expansion with $\mathbf{R}_j$ set at the O atom gives rise to a potential that resembles that of water much less closely (see SI).

These results encourage amending DCT to account for fluctuations in local quadrupole density. The approach we describe below for doing so is straightforward to generalize for higher-order multipoles. For the sake of generality, we therefore introduce the n^{th}-order multipole moment of a water molecule as

$$[\mathbf{\Gamma}^{(n)}]_{qrst\ldots} = \sum_{\alpha} q_\alpha [(\mathbf{r}_{j\alpha} - \mathbf{R}_j)^n]_{qrst\ldots} + \delta_{qr} a_{st\ldots} + \delta_{qs} a'_{rt\ldots} + \delta_{rs} a''_{qt\ldots} + \ldots \tag{11}$$

The constants a, a', a'', etc. are all arbitrary, since the moments $\mathbf{\Gamma}^{(n)}$ will always appear in contraction with tensors formed from gradients of the electrostatic Green's function. As with the quadrupole in Eq. 9, terms in $\mathbf{\Gamma}^{(n)}$ containing an identity in any two components (e.g. δ_{qr}) are therefore inconsequential. This contraction also makes the ordering of indices in $[\mathbf{\Gamma}^{(n)}]_{qrst\ldots}$ irrelevant.

C. Elaborating DCT

Extending DCT to describe higher-order multipoles could be accomplished most simply by adding a Gaussian quadrupole field $\mathbf{Q}_\mathbf{r}$. A natural choice for the generalized Hamiltonian,

$$\begin{aligned}\mathcal{H}_{\text{dip+quad}}[\mathbf{m}_\mathbf{r}, \mathbf{Q}_\mathbf{r}] = \mathcal{H}_{\text{dip}}[\mathbf{m}_\mathbf{r}] &+ \frac{1}{2\sigma_Q^2} \sum_{\mathbf{r}} \mathbf{Q}_\mathbf{r} : \mathbf{Q}_\mathbf{r} \\ &- \frac{1}{2} \sum_{\mathbf{r}} \sum_{\mathbf{r}'} \mathbf{Q}_\mathbf{r} : \left[\nabla\nabla\nabla \frac{1}{|\mathbf{r} - \mathbf{r}'|} \cdot \mathbf{m}_{\mathbf{r}'} \right. \\ &- \left. \frac{1}{4} \nabla\nabla\nabla\nabla \frac{1}{|\mathbf{r} - \mathbf{r}'|} : \mathbf{Q}_{\mathbf{r}'} \right] \end{aligned} \tag{12}$$

couples these fields through standard electrostatic interactions, providing a bias that renormalizes dipolar linear response. Though straightforward (and easily generalized to octupole density and hexadecapole moments, etc.), this approach is unsatisfying in several respects.

First, the electrostatic interaction between quadrupoles (and all higher-order multipoles) diverges at short range in a way that is not integrable in 3 dimensions, unlike the dipole-dipole interaction. The field theory defined by Eq. 12 would therefore require regularization, so that the parameter σ_Q sets a finite local quadrupole susceptibility. Second, and more importantly, this theory preserves the charge symmetry of standard DCT. Specifically, coupling to a charged solute gives a total energy

$$\mathcal{H}_{\text{dip+quad}} - \sum_{\mathbf{r}} \mathbf{E}_q(\mathbf{r}) \cdot \mathbf{m}_\mathbf{r} - \frac{1}{2} \sum_{\mathbf{r}} \nabla \mathbf{E}_q(\mathbf{r}) : \mathbf{Q}_\mathbf{r}$$

that is invariant to a simultaneous sign change of q, $\mathbf{m}_\mathbf{r}$, and $\mathbf{Q}_\mathbf{r}$. Just as for the Born model, ion solvation energies would remain even in solute charge q. Third, the number of degrees of freedom proliferates in such a generalization as higher order multipoles are included. At quadrupole order, the theory involves 12 scalar variables at each point in space. Imposing expected symmetries of $\mathbf{Q}_\mathbf{r}$ would reduce this number, but the fact remains that adding detail (in the form of higher-order multipoles) increases the theory's dimensionality. By contrast, an individual water molecule, modeled as a rigid body, possesses only 3 non-translational degrees of freedom, regardless of how exhaustively its electric potential $\phi(\mathbf{r})$ is expanded in multipole moments. These moments are not entirely independent variables; they are instead tied together by molecular geometry. Such constraints among molecular multipoles, we argue, are key to capturing charge asymmetry at a field theoretic level.

III. DEVELOPING A CHARGE ASYMMETRIC FIELD THEORY

A. Multipole constraints and dipolar response

The relationships among water's *molecular* multipoles can be easily understood. As an illustration, consider the dipole and quadrupole of an SPC/E water molecule. These moments are simply expressed in the coordinate system of Fig. 3a, $\boldsymbol{\mu} = \mu\hat{\boldsymbol{\mu}}$ and $\mathbf{K} = K\hat{\mathbf{x}}\hat{\mathbf{x}}$, where μ is the magnitude of the dipole vector, and K is a scalar constant. The unit vectors $\hat{\boldsymbol{\mu}}$ and $\hat{\mathbf{x}}$ point parallel and perpendicular, respectively, to the line of symmetry bisecting the hydrogen atoms. In the course of free molecular rotation, $\hat{\boldsymbol{\mu}}$ and $\hat{\mathbf{x}}$ can both explore the entire unit sphere, setting the range of possible realizations of $\boldsymbol{\mu}$ and $\mathbf{K}$. But if $\hat{\boldsymbol{\mu}}$ is fixed, $\hat{\mathbf{x}}$ can explore only a unit circle orthogonal to $\hat{\boldsymbol{\mu}}$, limiting the range of the tensor $\hat{\mathbf{x}}\hat{\mathbf{x}}$. Quadrupole fluctuations are thus partially constrained by the dipole's orientation, as are all higher-order moments.

We imagine that multipole density fields like $\mathbf{m}_\mathbf{r}$ and $\mathbf{Q}_\mathbf{r}$ represent a coarse-grained view on a material's molecular configuration. The coarse-graining procedure translates the constraint detailed above between each molecule's dipole $\boldsymbol{\mu}_j$ and its quadrupole $\mathbf{K}_j$ into a relationship between the fields $\mathbf{m}_\mathbf{r}$ and $\mathbf{Q}_\mathbf{r}$ – a connection that is less strict and more subtle than that between $\boldsymbol{\mu}_j$ and $\mathbf{K}_j$. We do not attempt here to detail this connection between coarse-grained fields. Instead, we focus on the

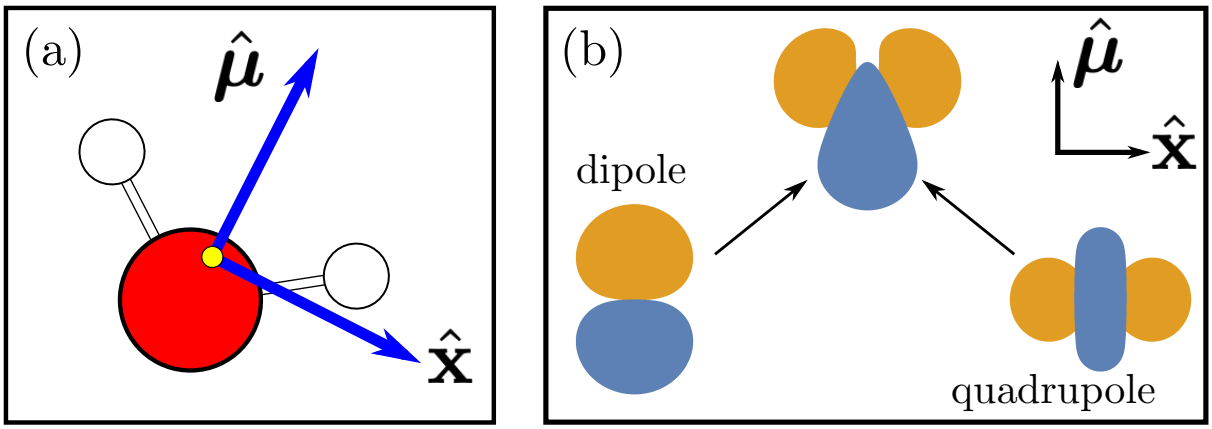

FIG. 3. The molecular structure of the water molecule gives rise to charge asymmetry. (a) The unit separation vector $\hat{\mathbf{x}}$ between the two hydrogen atoms is orthogonal to the unit dipole vector $\hat{\boldsymbol{\mu}}$. The yellow circle represents the multipole expansion point, i.e., the molecule's center of charge. (b) Equipotential surfaces of the molecular dipole and quadrupole. Summing contributions of these two lowest order moments (as indicated by the arrows and detailed in Eq. 10) is sufficient to generate a charge-asymmetric equipotential surface redolent of a water molecule.

molecular constraint's influence on the dipolar response of a single molecule. The result of this molecular calculation will then be used to motivate a modification of DCT.

1. Dipole statistics of an isolated molecule

Consider a single water molecule, at equilibrium, in an electric potential $\phi_{\rm ext}(\mathbf{r})$ that is generated by external charges. Taking the molecule's center of charge to be fixed at a position $\mathbf{R}_0$, a multipole expansion expresses its energy as

$$h(\hat{\boldsymbol{\mu}},\hat{\mathbf{x}}) = \sum_{n=1}^{\infty} \frac{1}{n!} \sum_{r,s,t,\ldots} [\boldsymbol{\Gamma}^{(n)}]_{rst\ldots} \frac{\partial}{\partial x_r}\frac{\partial}{\partial x_s}\frac{\partial}{\partial x_t}\ldots \phi_{\rm ext}(\mathbf{r})\Big|_{\mathbf{R}_0}, \tag{13}$$

where the $n^{\rm th}$ term of the expansion involves n spatial derivatives, indexed by $r,s,t,\ldots$. We have in mind a model with rigid intramolecular geometry, so that the unit vectors $\hat{\boldsymbol{\mu}}$ and $\hat{\mathbf{x}}$ specify the entire set of multipole moments $\boldsymbol{\Gamma}^{(n)}(\hat{\boldsymbol{\mu}},\hat{\mathbf{x}})$. We aim here to integrate over one intramolecular degree of freedom ($\hat{\mathbf{x}}$), while holding the other ($\hat{\boldsymbol{\mu}}$) fixed, to obtain a free energy

$$h_{\rm eff}(\hat{\boldsymbol{\mu}}) = -k_{\rm B}T \ln \int d\hat{\mathbf{x}}\, e^{-\beta h(\hat{\boldsymbol{\mu}},\hat{\mathbf{x}})} \tag{14}$$

that depends only on $\hat{\boldsymbol{\mu}}$. In doing so, we determine an effective energy $h_{\rm eff}(\hat{\boldsymbol{\mu}})$ for the molecular dipole in which fluctuations of all higher-order multipole moments have been taken into account, along with the constraints that relate them.

The integration in Eq. 14 is analytically intractable, even for this simplified single-molecule scenario. We therefore make a weak-field approximation,

$$h_{\rm eff} \approx \langle h \rangle_{\hat{\boldsymbol{\mu}}}^{\rm unbiased} = \sum_{n=1}^{\infty} \frac{1}{n!} \sum_{r,s,t,\ldots} [\langle \boldsymbol{\Gamma}^{(n)} \rangle_{\hat{\boldsymbol{\mu}}}^{\rm unbiased}]_{rst\ldots} \frac{\partial}{\partial x_r}\frac{\partial}{\partial x_s}\frac{\partial}{\partial x_t}\ldots \phi_{\rm ext}(\mathbf{r})\Big|_{\mathbf{R}_0}, \tag{15}$$

where $\langle\cdot\rangle_{\hat{\boldsymbol{\mu}}}^{\rm unbiased}$ denotes an unbiased orientational average over $\hat{\mathbf{x}}$ subject to the constraint of fixing $\hat{\boldsymbol{\mu}}$. We further assume that the potential $\phi_{\rm ext}(\mathbf{r})$ is slowly varying, so that the sum over n can be truncated at low order. To be sure, these assumptions are quantitatively lacking for a liquid environment, which generates strong electric fields that vary significantly on the scale of a single molecule. We employ them here in order to capture the lowest-order influence of quadrupole (or octupole, etc.) fluctuations on the statistics of molecular polarization.

The symmetry of a water molecule causes many elements of $\boldsymbol{\Gamma}^{(n)}$ to vanish, regardless of the specific model considered. The irrelevance of isotropic contributions (e.g., terms in $\mathbf{K}$ that are proportional to $\mathbf{I}$) causes many other multipole elements to be unimportant. Furthermore, the contraction in Eq. 13 allows the indices of $[\boldsymbol{\Gamma}^{(n)}]_{rst\ldots}$ to be permuted arbitrarily. As a result, the class of elements relevant to h at a given multipole or-

der is not large. Nontrivial contributions to $\mathbf{\Gamma}^{(n)}$ can all be written in terms of dyadic products involving an even number $2m$ of factors $\hat{\mathbf{x}}$ together with $n-2m$ factors of $\hat{\boldsymbol{\mu}}$ (e.g., $\hat{\boldsymbol{\mu}}\hat{\boldsymbol{\mu}}$ and $\hat{\mathbf{x}}\hat{\mathbf{x}}$ at order $n=2$, $\hat{\boldsymbol{\mu}}\hat{\boldsymbol{\mu}}\hat{\boldsymbol{\mu}}$ and $\hat{\boldsymbol{\mu}}\hat{\mathbf{x}}\hat{\mathbf{x}}$ at order $n=3$, etc.). Relevant contributions to the *average* moments $\langle\mathbf{\Gamma}^{(n)}\rangle_{\hat{\boldsymbol{\mu}}}^{\text{unbiased}}$ in Eq. 15 then follow from results of straightforward angular integration:

$$\begin{aligned}\langle\hat{\mathbf{x}}\hat{\mathbf{x}}\rangle_{\hat{\boldsymbol{\mu}}}^{\text{unbiased}} &= \frac{1}{2}(\mathbf{I}-\hat{\boldsymbol{\mu}}\hat{\boldsymbol{\mu}}),\\ \langle\hat{\mathbf{x}}\hat{\mathbf{x}}\hat{\mathbf{x}}\hat{\mathbf{x}}\rangle_{\hat{\boldsymbol{\mu}}}^{\text{unbiased}} &= \frac{3}{8}(\mathbf{I}-\hat{\boldsymbol{\mu}}\hat{\boldsymbol{\mu}})(\mathbf{I}-\hat{\boldsymbol{\mu}}\hat{\boldsymbol{\mu}}), \qquad \dots \end{aligned} \tag{16}$$

where we have exploited the arbitrariness of index ordering in $[\langle\mathbf{\Gamma}^{(n)}\rangle_{\hat{\boldsymbol{\mu}}}^{\text{unbiased}}]_{rst\dots}$. Removing isotropic contributions that vanish when contracted with gradients of $\phi_{\text{ext}}(\mathbf{r})$, we finally obtain an effective dipolar energy

$$h_{\text{eff}} \approx \sum_{n=1} b_n(\boldsymbol{\mu}\cdot\nabla)^n\phi_{\text{ext}}(\mathbf{r})\Big|_{\mathbf{R}_0} \tag{17}$$

The form of this result is general for any SPC model that has the symmetry of a water molecule. The values of coefficients b_n, on the other hand, are model-specific; they are also sensitive to the choice of reference point $\mathbf{R}_0$ defining the multipole expansion. For the case of SPC/E water and $\mathbf{R}_0$ set at the molecule's center of charge, $b_1 = 1$ and $b_2 \approx -0.6e^{-1}$.

In constructing a field theory in the next section, we will focus on a truncation of the sum in Eq. 17 at $n=2$,

$$h_{\text{eff}}^{(2)}(\boldsymbol{\mu}) = \boldsymbol{\mu}\cdot\nabla\phi_{\text{ext}} + b_2(\boldsymbol{\mu}\cdot\nabla)^2\phi_{\text{ext}} \tag{18}$$

The first term in $h_{\text{eff}}^{(2)}$ describes direct electrostatic coupling between the molecular dipole and an electric field external to that molecule. Its coarse-grained analog, appearing explicitly in Eq. 3 and implicitly in Eq. 2 through the dipole-dipole interaction, defines the nonlocal interaction energy in DCT. Correspondingly, this contribution is charge symmetric – a potential $\phi_{\text{ext}} = q/r$ due to an external point charge yields an energy that is invariant to inverting the signs of both q and $\boldsymbol{\mu}$.

The second term in $h_{\text{eff}}^{(2)}$, by contrast, breaks charge symmetry – it effects response to an external point charge that is not equivalent for $q>0$ and $q<0$. This nonlinear contribution originates in fluctuations of $\hat{\mathbf{x}}$, which dictates the molecular quadrupole. By integrating out quadrupole fluctuations, we have thus obtained an effective dipolar energy that reflects the asymmetric charge distribution within a water molecule.

Carrying out the summation in Eq. 17 to higher order generates a series of charge symmetric (n odd) and charge antisymmetric (n even) terms. If a particular model and choice of $\mathbf{R}_0$ gives $b_2 = 0$ (as is the case for SPC/E water if one chooses the oxygen atom as the reference point), charge asymmetry would emerge first at hexadecapole order ($n=4$). If a particular model features a completely charge-symmetric intramolecular geometry (e.g., BNS water[46]) and $\mathbf{R}_0$ is set at the center of charge, then $b_n = 0$ for all even values of n, so that h_{eff} is appropriately equivalent for cation and anion response.

B. A constraint-inspired field theory

The analysis of single-molecule response we have presented suggests important considerations for generalizing DCT. Foremost, it indicates that the introduction of quadrupolar fields (or other higher-order multipole moments), as in Eq. 12, should be accompanied by consideration of constraints dictated by molecular geometry. The nature of these constraints is clear at the molecular level, but an appropriate expression in terms of coarse-grained fields like $\mathbf{m}_\mathbf{r}$ and $\mathbf{Q}_\mathbf{r}$ is not obvious. If one were to impose strict constraints, such as $\mathbf{m}_\mathbf{r}\cdot\mathbf{Q}_\mathbf{r} = 0$ at each position $\mathbf{r}$, then partition functions and response functions could be formulated from Eq. 12 using methods that have proven effective in other contexts.[28,47] This approach would be analytically challenging, however, since the nonlinear constraints we have described prevent mapping onto a Gaussian theory simply by introducing auxiliary fields as in Refs. 28 and 47.

We will follow a different approach. Rather than taking the constraints themselves from a molecular model, we instead take the effective dipolar energy (Eq. 18) they imply when local quadrupole fluctuations are integrated out. In doing so, we neglect correlated fluctuations in the quadrupole field, in effect treating $\mathbf{Q}_\mathbf{r}$ and $\mathbf{Q}_{\mathbf{r}'}$ (with $\mathbf{r}\neq\mathbf{r}'$) as independent variables for a given realization of the dipole field. Focusing in this way on quadrupolar response to $\mathbf{m}_\mathbf{r}$ alone conforms to the spirit of the multipole expansion on which our perspective is based. The resulting charge-asymmetric, field-theoretic Hamiltonian follows from Eq. 18,

$$\mathcal{H}[\mathbf{m}_\mathbf{r}] = \mathcal{H}_{\text{dip}}[\mathbf{m}_\mathbf{r}] - \sum_\mathbf{r}\mathbf{E}_q(\mathbf{r})\cdot\mathbf{m}_\mathbf{r} - b\sum_\mathbf{r}\mathbf{m}_\mathbf{r}\,\mathbf{m}_\mathbf{r}:\nabla\mathbf{E}(\mathbf{r}) \tag{19}$$

where $\mathbf{E} = \mathbf{E}_q + \mathbf{E}_{\text{dip}}$ is the total electric field at $\mathbf{r}$, including contributions from the solute and from the dipole field,

$$\mathbf{E}_{\text{dip}}(\mathbf{r}) = -\sum_{\mathbf{r}'}\nabla\nabla'\frac{1}{|\mathbf{r}-\mathbf{r}'|}\cdot\mathbf{m}'_\mathbf{r}$$

We will not attempt here to derive or motivate a value for the parameter b, whose connection to the molecular parameter b_2 is conceptually but not quantitatively clear.

Eq. 19 is the central result of this paper. It defines a field theory that is charge asymmetric in accord with the asymmetric response of an isolated water molecule. It respects the rotational symmetry of the liquid state and is simple to express, but its nonlinearity and spatial nonlocality make analysis unwieldy. To make exploratory progress, we introduce two additional approximations. First, we replace the fluctuating total electric field in Eq. 19 with a constant, screened external field, $\mathbf{E}(\mathbf{r}) \approx \mathbf{E}_q/\epsilon$, that would result on average from linear dielectric response. This replacement removes a nonlinearity of third order in the dipole field, while preserving nonlinear *response* to the solute's charge. It also lim-

its the complications we have added to a spatially local functional of the field $\mathbf{m_r}$.

With this simplification, the Hamiltonian in Eq. 19 becomes bilinear in the dipole field, whose statistics are therefore Gaussian. Analysis remains challenging, however, because the effective dipolar coupling generates localized normal modes that are not easily anticipated. The fluctuation spectrum of $\mathbf{m_r}$ thus changes as $\mathbf{E}_q$ is introduced, producing a complicated nonlinear response that breaks charge symmetry. We simplify further by taking a variational approach, introducing a more tractable reference system

$$\mathcal{H}_{\rm ref}[\mathbf{m_r}] = \mathcal{H}_{\rm dip}[\mathbf{m_r}] + \tilde{q}\sum_{\mathbf{r}} \mathbf{m_r}\cdot\nabla r^{-1} \qquad (20)$$

$\mathcal{H}_{\rm ref}$ describes the response of a conventional dielectric continuum to a solute with *effective* charge $\tilde{q}$.

We determine an optimal choice of the variational parameter $\tilde{q}$ from the Gibbs-Bogoliubov bound,

$$\ln \mathcal{Z} \geq \ln \mathcal{Z}_{\rm ref} - \beta\langle\Delta\mathcal{H}\rangle_{\rm ref}$$

on the partition function $\mathcal{Z}$ and its counterpart $\mathcal{Z}_{\rm ref}$ for the reference system. Here, $\Delta\mathcal{H} = \mathcal{H} - \mathcal{H}_{\rm ref}$, and $\langle\cdot\rangle_{\rm ref}$ denotes an ensemble average in the reference system. Evaluating $\langle\Delta\mathcal{H}\rangle_{\rm ref}$ requires calculating, and appropriately summing, both $\langle\mathbf{m_r}\rangle_{\rm ref}$ and $\langle\mathbf{m_r}\mathbf{m_r}\rangle_{\rm ref}$. The former, $\langle\mathbf{m_r}\rangle_{\rm ref} = \mathbf{E}_q(\epsilon-1)/(4\pi\epsilon)$ is simple to compute and manipulate, both on- and off-lattice. The latter involves the response function $\chi(\mathbf{r},\mathbf{r}') = \langle\delta\mathbf{m_r}\delta\mathbf{m_{r'}}\rangle_{\rm ref}$, where $\delta\mathbf{m_r} = \mathbf{m_r} - \langle\mathbf{m_r}\rangle_{\rm ref}$. In the presence of a volume-excluding solute, $\chi(\mathbf{r},\mathbf{r}')$ is generally complicated, and in the off-lattice case it is singular for $\mathbf{r} = \mathbf{r}'$. But with space treated discretely it can be written compactly for a solute that occupies a single lattice cell. Placing this solute at the origin, we have[28]

$$\chi(\mathbf{r},\mathbf{r}') = -\frac{3v^3}{\beta\epsilon(2\epsilon+1)}\left(\frac{\epsilon-1}{4\pi}\right)^3 \nabla\nabla\frac{1}{r}\cdot\nabla\nabla\frac{1}{r}$$

for $\mathbf{r} \neq 0$. Approximating sums $\sum_{\mathbf{r}\neq 0}$ as integrals $v^{-1}\int_{r<R} d\mathbf{r}$, we obtain

$$\tilde{q} = \frac{q}{1+Bq}$$

with $B = -b(v/R^3)(\epsilon-1)/(4\pi\epsilon)$, and

$$\begin{aligned} F_{\rm chg}^{(\rm var)}(q) &\approx F_{\rm chg}^{(\rm ref)}(q) + \langle\Delta\mathcal{H}\rangle_{\rm ref} \\ &= -\frac{q\tilde{q}}{2R}\frac{\epsilon-1}{\epsilon} - \frac{3bqk_{\rm B}T}{2\pi^2\epsilon}\frac{(\epsilon-1)^3}{2\epsilon+1}. \end{aligned} \qquad (21)$$

For simplicity we have taken $R = v^{1/3}/2$. Reasonable alternatives, such as $R = (3v/4\pi)^{1/3}$ yield similar results.

Eq. 21 includes a term linear in q, whose coefficient could be regarded as a contribution to the neutral cavity potential $\langle V\rangle_0$. Since we have made no attempt to include contributions from distant interfaces, this term cannot offer a full accounting of charge asymmetry in the limit $q \to 0$. In the same spirit as the modified Born model in Eq. 5, we could replace it with the correct neutral cavity potential,

$$F_{\rm chg}^{(\rm var)}(q;\langle V\rangle_0) \approx -\frac{q\tilde{q}}{2R}\frac{\epsilon-1}{\epsilon} + q\langle V\rangle_0. \qquad (22)$$

This modification is only significant at very small values of q. Predictions for fully charged ions ($q = \pm e$) are essentially unaffected.

IV. NUMERICAL RESULTS

Predictions of the variational result in Eq. 22 depend on input parameters R and b, which set the effective solute size and the strength of nonlinearity due to quadrupole fluctuations. We will treat these parameters as we did the dielectric radius R of the Born model in Sec. II A. Specifically, we require consistency across ions with a given volume-excluding radius R_0 but otherwise adjust R and b to obtain the best possible agreement with results from molecular simulation.

For any physically well-founded theory, we expect the optimal choice of dielectric radius R to be similar, but not necessarily identical, to the radius R_0 of molecular volume exclusion. Indeed, Fig. 4a shows that R for our nonlinear variational theory depends on R_0 in almost precisely the same way as for the Born model. Across the range of solute sizes considered, we find that dielectric and volume-excluding radii differ by a nearly constant offset, $R \approx R_0 - 1.31\,\text{Å}$. With this offset, R corresponds suggestively to the distance of closest approach between the solute and the hydrogen atoms of surrounding water molecules, as shown in Fig. 4b for $q = -e$ and $R_0 = 3.17\,\text{Å}$ (examples for different choices of R_0 are given in the SI). The idea that an optimal dielectric radius may appear smaller than R_0 owing to the longer reach of water's hydrogen atoms has been proposed and discussed before,[19–21] but for the specific case of negatively charged solutes, whose solvation favors molecular orientations that place hydrogen atoms as close to the solute as possible. In our case, we stress that the same dielectric radius is used for cations and anions that have the same volume-excluding size. Charge asymmetry is an emergent, rather than engineered, feature of this approach.

Because the optimal choice of R aligns closely with that of the Born model, we view the nonlinear theory of Eq. 19 as adding a single adjustable parameter, namely b. We anticipate that b, which has units of inverse charge, should be roughly of order $1/e$. We also expect that b should decay in magnitude as solute size R_0 increases, both because near-field contributions are less prominent for large ions and because linear response theory is already successful in this limit. The origin of b in constraints of molecular geometry, which are not at all transparent at a field-theoretic level, makes it difficult to de-

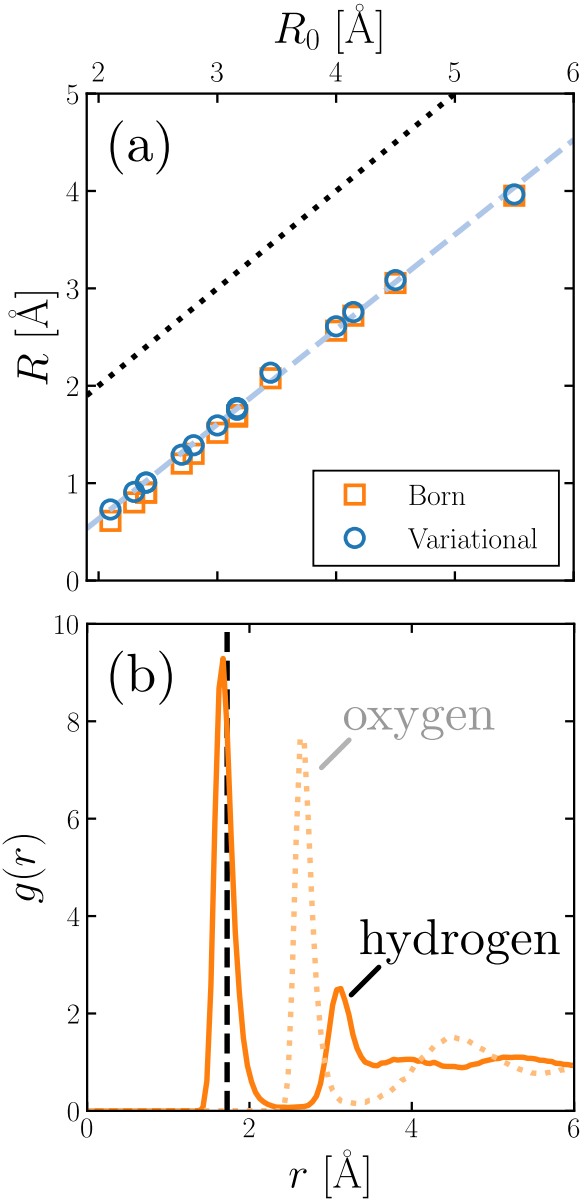

FIG. 4. The optimal dielectric radius R is generally smaller than the radius R_0 of a solute's excluded volume. (a) The relationship between R and R_0, determined by fitting theoretical results to computer simulations, is approximately linear. The dotted line indicates $R = R_0$, and the dashed line shows $R \approx 0.97R_0 - 1.31\,\text{Å}$. Results are shown for the Born model (Eq. 5) and for our variational theory (Eq. 22). (b) The solute-solvent radial distribution function [$g(r)$] suggests R roughly corresponds to the distance of closest approach of water's hydrogen atoms to the solute. Solid and dotted lines show solute-hydrogen $g(r)$ and solute-oxygen $g(r)$, respectively, for $R_0 = 3.17\,\text{Å}$ and $q = -e$. The vertical dashed line indicates the best-fit value of R for this solute size.

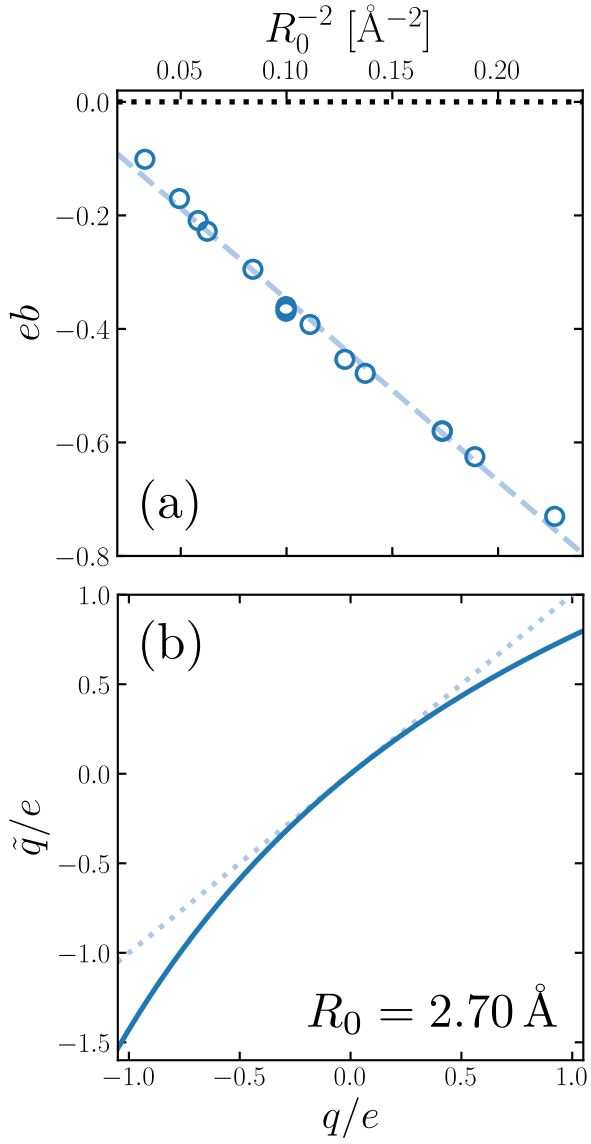

FIG. 5. (a) The nonlinearity parameter b (see Eq. 19), determined by fitting theoretical results to computer simulations, varies linearly with R_0^{-2}. The dashed line shows $eb = -0.03 - 3.20R_0^{-2}$. (b) The resulting effective variational charge $\tilde{q}$ is greater in magnitude for anions than it is for cations, as shown for a solute with volume excluding radius $R_0 = 2.70\,\text{Å}$ (solid line). The dotted line indicates $\tilde{q} = q$.

velop further *a priori* expectations. Maximizing agreement of Eq. 22 with simulation results for $F_{\text{chg}}(q)$, we find empirically that $b \approx e^{-1}(-0.03 - 3.20R_0^{-2})$ to a very good approximation, as shown in Fig. 5a. As a practical matter, this simple and quantitatively successful fit allows accurate application of the variational result in Eq. 22 to arbitrary R_0 without any further fitting. Physically, the observed scaling of b with R_0 is intriguing, but we cannot offer a compelling explanation.

With these fitted values of R and b, the effective variational charge $\tilde{q}$ is larger in magnitude for $q = -e$ than for $q = e$, as shown in Fig. 5b for a solute with volume excluding raduis $R_0 = 2.70\,\text{Å}$. The resulting charge asymmetry therefore favors solvation of fully charged anions over cations with the same volume-excluding size, as ob-

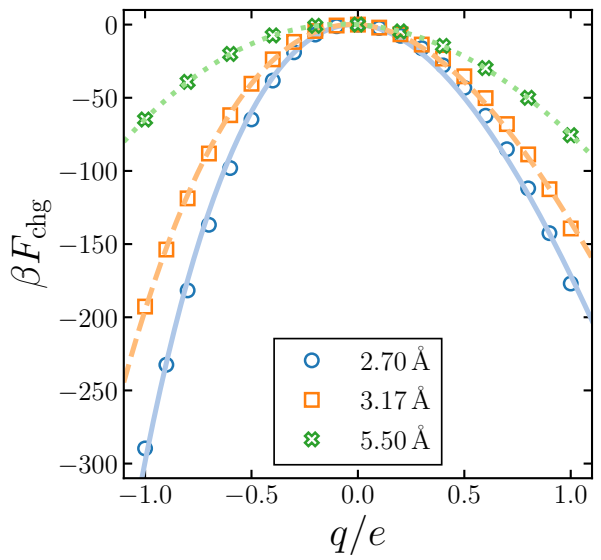

FIG. 6. Solute charging free energy $F_{\rm chg}^{\rm (var)}$ estimated from the approximate variational solution to our nonlinear field theory, for different solute sizes R_0 as indicated in the legend. Symbols show results from simulations. Lines indicate best fits of $F_{\rm chg}^{\rm (var)}$ (Eq. 22) to the simulation results. For smaller solute sizes, $F_{\rm chg}^{\rm (var)}$ significantly improves upon $F_{\rm chg}^{\rm (Born)}$, especially for $q = \pm e$ (see Fig. 1 and SI).

served in computer simulations. Fig. 6 shows a detailed comparison of charging free energies obtained from simulation and from the nonlinear variational theory. For all solute sizes considered, and across the entire range $q = -e$ to $q = e$, the agreement is excellent. For the largest solute, $R_0 = 5.5\,\text{Å}$, there is little room for improvement over the linear response prediction Eq. 5; a small but noticeable charge-asymmetric response in simulation results is nonetheless captured well by our variational result. For the smaller solutes, $R_0 = 2.7\,\text{Å}$ and $R_0 = 3.17\,\text{Å}$, improvement over the Born model is dramatic. Discrepancies between simulation and the nonlinear field theory result certainly remain, but the qualitative shortcomings of DCT have essentially been erased.

V. DISCUSSION AND OUTLOOK

Our aim in this article has been to address a key failing of DCT – a fundamental lack of charge asymmetry in ion solvation – while preserving its conceptual simplicity. Motivated by the influence of molecular quadrupole fluctuations on the statistics of polarization, the effective Hamiltonian presented in Eq. 19 adds the kind of sensitivity to nonlinear response that is required to capture charge-asymmetric solvation. Our approximate solution to this model, obtained by a variational procedure, gives a charging free energy (Eq. 22) with the same basic form as the standard Born model (Eq. 5), but with an effective ion charge that is renormalized by nonlinear response. Setting the strength b of the nonlinearity to be a simple function of ion size, we obtain close quantitative agreement with results of computer simulations.

While we believe our approach is original, it is certainly not the only way to achieve charge asymmetric solvation energies. In many previous efforts, asymmetry was introduced by hand. Latimer, Pitzer and Slansky[19] amended the Born model by assigning different dielectric radii for anions and cations of the same size, an approach that has been adopted in subsequent theoretical studies. The piecewise-affine response model[21] of Bardhan *et al.* follows a similar spirit, empirically adjusting the nature of electrostatic response as a solute's charge is varied. We recently demonstrated that an analogous treatment of interfacial solvation performs reasonably well in describing ion-specific adsorption to the air-water surface.[15] In all these approaches, charge asymmetry was built in *a posteriori*, whereas it is an emergent feature of the model defined by Eq. 19.

Fluctuations in a solvent's polarization and in its density are both advanced at microscopic scales by rearrangement of discrete molecular structures; they are therefore tied together intimately. In this paper we have taken an electrostatic perspective on the nonlinear response to solute charging, in which polarization fluctuations are renormalized by degrees of freedom that can be described in terms of electrostatic multipoles. Polarization statistics can of course also be complicated by the influence of microscopic density fluctuations, as highlighted by the sensitivity of dielectric susceptibility to volume exclusion.[28] Work by Dinpajooh and Matyushov[48] emphasizes that these biases are not completely distinct, suggesting the interesting possibility that the quadrupole-mediated response we have analyzed might be conceived alternatively in terms of microscopic density fluctuations.

More generally, the interplay between density and polarization response generates a spectrum of solvation behaviors, ranging from hydrophobic effects at one extreme to small ion solvation at the other. A lack of theoretical methods and tractable models that successfully span this range stands as a one of the most severe challenges limiting computational biophysics and nanoscience. While research on hydrophobic effects remains active,[49] field theoretic approaches to the underlying density fluctuations have matured greatly in recent years.[8,50–53] The powerful tools they provide do not yet have counterparts in an electrostatic context, a gap that our work seeks to help fill. While much remains to be done in refining the nonlinear theory we have formulated and in developing practical methods to solve it, the work presented here is in our view a meaningful step towards placing theories for electrostatic and hydrophobic solvation on comparable footing. As such, it advances the development of efficient computational techniques that apply across the entire hydrophobic/hydrophilic spectrum.

VI. METHODS

All simulations used the SPC/E water model[17] and were performed with the LAMMPS simulation package.[54] Simulations comprised 64, 256 or 512 water molecules plus a single solute, such that the total number density was $\rho = 0.03333\,\text{Å}^{-3}$. Our model solute is a Lennard-Jones particle,

$$u(r) = 4\varepsilon[(R_0/r)^{12} - (R_0/r)^6], \tag{23}$$

where r is the distance between the center of the solute (where the solute charge is also located) and the oxygen atom of the water molecule. We set $\varepsilon = 0.1553\,\text{kcal/mol}$ (the same as SPC/E water) for all solutes investigated, but varied R_0 as indicated throughout the manuscript. Full 3D periodic boundary conditions with particle-particle particle-mesh Ewald summation was used throughout,[55,56] with a homogeneous background charge to neutralize the system. Simulations of 5 ns in length, with a periodic cell of side length L, were performed with $q/e = -1.0, -0.9, \ldots, +0.9, +1.0$. (For $R_0 \geq 4.5\,\text{Å}$ we used $q/e = -1.0, -0.8, \ldots, +0.8, +1.0$). The charging free energy $F_{\text{chg}}^{(L)}$ was then computed using the MBAR algorithm,[57] as described previously in Ref 44. The quantity $F_{\text{chg}}^{(L)}$ suffers from severe finite size effects. It has previously been shown[34,43,44] that the quantity,

$$F_{\text{chg}} = F_{\text{chg}}^{(L)} + \frac{q}{2}\left(\frac{\epsilon - 1}{\epsilon}\right)\phi_{\text{wig}} + qV_{\text{surf}} \tag{24}$$

accurately estimates the macroscopic limit $L \to \infty$, including the effects of distant interfaces. In Eq. 24, the Wigner potential ϕ_{wig}/q is defined as the electrostatic potential at the site of a unit point charge due to all of its periodic replicas and a homogeneous background charge that acts to neutralize the primitive cell. The surface potential $V_{\text{surf}} = -590\,\text{mV}$[14] was determined by numerically integrating the solvent's charge density profile $\langle\rho_{\text{solv}}(z)\rangle$ according to $V_{\text{surf}} = 4\pi\int_{z_{\text{vap}}}^{z_{\text{liq}}} \text{d}z\,\langle\rho_{\text{solv}}(z)\rangle z$, where z_{liq} and z_{vap} denote locations on either side of a neat liquid/vapor interface. Nonlinear curve fitting to obtain optimal choices of R and b (see Eqs. 5 and 22) was performed using the True Region Reflective algorithm,[58] as implemented in SciPy's 'curve_fit' routine.[59]

ACKNOWLEDGMENTS

S.J.C (02/15 to 09/17) and P.L.G were supported by the U.S. Department of Energy, Office of Basic Energy Sciences, through the Chemical Sciences Division (CSD) of Lawrence Berkeley National Laboratory (LBNL), under Contract DE-AC02-05CH11231. K.K.M is supported by Director, Office of Science, Office of Basic Energy Sciences, of the U.S. Department of Energy under contract No. DEAC02-05CH11231. From 10/17 to 02/21, S.J.C. was supported by a Royal Commission for the Exhibition of 1851 Research Fellowship.

DATA AVAILABILITY STATEMENT

The data that supports the findings of this study are available within the article and its supplementary material. Data for the charging free energies and a Python analysis script are openly available at the University of Cambridge Data Repository, `https://doi.org/10.17863/CAM.66169`.

[1] K. Tielrooij, N. Garcia-Araez, M. Bonn, and H. Bakker, Science **328**, 1006 (2010).
[2] D. E. Otten, P. R. Shaffer, P. L. Geissler, and R. J. Saykally, Proc. Natl. Acad. Sci. USA **109**, 701 (2012).
[3] D. Verreault, W. Hua, and H. C. Allen, J. Phys. Chem. Lett. **3**, 3012 (2012).
[4] L. Piatkowski, Z. Zhang, E. H. Backus, H. J. Bakker, and M. Bonn, Nature Commun. **5**, 4083 (2014).
[5] D. L. McCaffrey, S. C. Nguyen, S. J. Cox, H. Weller, A. P. Alivisatos, P. L. Geissler, and R. J. Saykally, Proc. Natl. Acad. Sci. USA **114**, 13369 (2017).
[6] Y. Chen, H. I. Okur, N. Gomopoulos, C. Macias-Romero, P. S. Cremer, P. B. Petersen, G. Tocci, D. M. Wilkins, C. Liang, M. Ceriotti, and S. Roke, Sci. Adv. **2**, e1501891 (2016).
[7] G. Hummer, L. R. Pratt, and A. E. García, J. Phys. Chem. A **102**, 7885 (1998).
[8] K. Lum, D. Chandler, and J. D. Weeks, J. Phys. Chem. B **103**, 4570 (1999).
[9] H. S. Ashbaugh, J. Phys. Chem. B **104**, 7235 (2000).
[10] D. Horinek and R. R. Netz, Phys. Rev. Lett. **99**, 226104 (2007).
[11] Y. Levin, Phys. Rev. Lett. **102**, 147803 (2009).
[12] D. Ben-Amotz, J. Phys.: Condens. Matter **28**, 414013 (2016).
[13] T. L. Beck, Chem. Phys. Lett. **561**, 1 (2013).
[14] R. C. Remsing, M. D. Baer, G. K. Schenter, C. J. Mundy, and J. D. Weeks, J. Phys. Chem. Lett. **5**, 2767 (2014).
[15] S. J. Cox, D. G. Thorpe, P. R. Shaffer, and P. L. Geissler, Chem. Sci. **11**, 11791 (2020).
[16] M. Born, Zeitschrift für Physik **1**, 45 (1920).
[17] H. J. C. Berendsen, J. R. Grigera, and T. P. Straatsma, J. Phys. Chem. **91**, 6269 (1987).
[18] J. Tomasi, B. Mennucci, and R. Cammi, Chem. Rev. **105**, 2999 (2005).
[19] W. M. Latimer, K. S. Pitzer, and C. M. Slansky, J. Chem. Phys. **7**, 108 (1939).
[20] S. Rajamani, T. Ghosh, and S. Garde, J. Chem. Phys. **120**, 4457 (2004).
[21] J. P. Bardhan, P. Jungwirth, and L. Makowski, J. Chem. Phys. **137**, 124101 (2012).
[22] R. A. Marcus, J. Chem. Phys. **24**, 966 (1956).
[23] G. Hummer, L. R. Pratt, and A. E. García, J. Am. Chem. Soc. **119**, 8523 (1997).
[24] L. R. Pratt and R. A. LaViolette, Mol. Phys. **94**, 909 (1998).
[25] T. L. Beck, M. E. Paulaitis, and L. R. Pratt, *The Potential Distribution Theorem and Models of Molecular Solutions* (Cambridge University Press, Cambridge, United Kingdom, 2012).
[26] T. T. Duignan, M. D. Baer, G. K. Schenter, and C. J. Mundy, Chem. Sci. **8**, 6131 (2017).
[27] T. T. Duignan, M. D. Baer, G. K. Schenter, and C. J. Mundy, J. Chem. Phys. **147**, 161716 (2017).
[28] X. Song, D. Chandler, and R. Marcus, J. Phys. Chem. **100**, 11954 (1996).
[29] P. Madden and D. Kivelson, "A consistent molecular treatment of dielectric phenomena," in *Adv. Chem. Phys.* (John Wiley & Sons, Inc., 1984) pp. 467–566.

[30]V. Ballenegger and J.-P. Hansen, J. Chem. Phys **122**, 114711 (2005).
[31]A. Schlaich, E. W. Knapp, and R. R. Netz, Phys. Rev. Lett. **117**, 048001 (2016).
[32]P. Loche, C. Ayaz, A. Schlaich, D. J. Bonthuis, and R. R. Netz, J. Phys. Chem. Lett. **9**, 6463 (2018).
[33]C. Zhang and M. Sprik, Phys. Chem. Chem. Phys. **22**, 10676 (2020).
[34]G. Hummer, L. R. Pratt, and A. E. García, J. Phys. Chem. **100**, 1206 (1996).
[35]J. Åqvist and T. Hansson, J. Phys. Chem. B **102**, 3837 (1998).
[36]E. Harder and B. Roux, J. Chem. Phys. **129**, 234706 (2008).
[37]A. Arslanargin and T. L. Beck, J. Chem. Phys. **136**, 104503 (2012).
[38]L. Horváth, T. Beu, M. Manghi, and J. Palmeri, J. Chem. Phys. **138**, 154702 (2013).
[39]R. C. Remsing and J. D. Weeks, J. Phys. Chem. B **120**, 6238 (2016).
[40]C. C. Doyle, Y. Shi, and T. L. Beck, J. Phys. Chem. B **123**, 3348 (2019).
[41]R. Lynden-Bell and J. Rasaiah, J. Chem. Phys. **107**, 1981 (1997).
[42]F. Figueirido, G. S. Del Buono, and R. M. Levy, J. Chem. Phys. **103**, 6133 (1995).
[43]P. H. Hünenberger and J. A. McCammon, J. Chem. Phys. **110**, 1856 (1999).
[44]S. J. Cox and P. L. Geissler, J. Chem. Phys. **148**, 222823 (2018).
[45]S. J. Cox, Proc. Natl. Acad. Sci. **117**, 19746 (2020).
[46]F. H. Stillinger and A. Rahman, J. Chem. Phys. **60**, 1545 (1974).
[47]D. Chandler, Phys. Rev. E **48**, 2898 (1993).
[48]M. Dinpajooh and D. V. Matyushov, J. Chem. Phys. **143**, 044511 (2015).
[49]L. R. Pratt, M. I. Chaudhari, and S. B. Rempe, J. Phys. Chem. B **120**, 6455 (2016).
[50]D. Chandler, Nature **437**, 640 (2005).
[51]P. Varilly, A. J. Patel, and D. Chandler, J. Chem. Phys. **134**, 074109 (2011).
[52]S. Vaikuntanathan and P. L. Geissler, Phys. Rev. Lett. **112**, 020603 (2014).
[53]S. Vaikuntanathan, G. Rotskoff, A. Hudson, and P. L. Geissler, Proc. Natl. Acad. Sci. USA **113**, E2224 (2016).
[54]S. Plimpton, J. Comput. Phys. **117**, 1 (1995).
[55]R. W. Hockney and J. W. Eastwood, *Computer simulation using particles* (CRC Press, 1988).
[56]J. Kolafa and J. W. Perram, Mol. Sim. **9**, 351 (1992).
[57]M. R. Shirts and J. D. Chodera, J. Chem. Phys. **129**, 124105 (2008).
[58]M. A. Branch, T. F. Coleman, and Y. Li, SIAM J. Sci. Comput. **21**, 1 (1999).
[59]A. Vijaykumar, A. P. Bardelli, A. Rothberg, A. Hilboll, A. Kloeckner, A. Scopatz, A. Lee, A. Rokem, C. N. Woods, C. Fulton, C. Masson, C. Häggström, C. Fitzgerald, D. A. Nicholson, D. R. Hagen, D. V. Pasechnik, E. Olivetti, E. Martin, E. Wieser, F. Silva, F. Lenders, F. Wilhelm, G. Young, G. A. Price, G.-L. Ingold, G. E. Allen, G. R. Lee, H. Audren, I. Probst, J. P. Dietrich, J. Silterra, J. T. Webber, J. Slavič, J. Nothman, J. Buchner, J. Kulick, J. L. Schönberger, J. V. de Miranda Cardoso, J. Reimer, J. Harrington, J. L. C. Rodríguez, J. Nunez-Iglesias, J. Kuczynski, K. Tritz, M. Thoma, M. Newville, M. Kümmerer, M. Bolingbroke, M. Tartre, M. Pak, N. J. Smith, N. Nowaczyk, N. Shebanov, O. Pavlyk, P. A. Brodtkorb, P. Lee, R. T. McGibbon, R. Feldbauer, S. Lewis, S. Tygier, S. Sievert, S. Vigna, S. Peterson, S. More, T. Pudlik, T. Oshima, T. J. Pingel, T. P. Robitaille, T. Spura, T. R. Jones, T. Cera, T. Leslie, T. Zito, T. Krauss, U. Upadhyay, Y. O. Halchenko, and Y. Vázquez-Baeza, Nat. Methods **17**, 261 (2020).

Supporting Information

S1. THE EFFECT OF INCLUDING $\langle V\rangle_0$ ON $F_{\mathrm{chg}}^{(\mathrm{Born})}$

In Fig. S1 we present the results of including a term $q\langle V\rangle_0$ in the Born model of solvation (Eq. 5). On the scale of Fig. S1, this has negligible impact on $F_{\mathrm{chg}}^{(\mathrm{Born})}$. As seen in the insets of Fig. S1, the effect of including $q\langle V\rangle_0$ is most pronounced for small q.

S2. CONTRIBUTIONS FROM MORE DISTANT SOLVATION SHELLS

Fig. S2 shows $\langle V_{\mathrm{near}}^{(2)}\rangle_q$ and $\langle V_{\mathrm{near}}^{(3)}\rangle_q$, the contributions to $\langle V\rangle_q$ from the second and third solvation shells, respectively, for the same system shown in Fig. 2 in the main text. Denoting the distance between the center of the solute and the oxygen atom of a water molecule as R_{SO}, a molecule is deemed to be in the second coordination shell if $3.5\,\text{Å} < R_{\mathrm{SO}} \leq 5.5\,\text{Å}$, and within the third coordination shell if $5.5\,\text{Å} < R_{\mathrm{SO}} \leq 8.5\,\text{Å}$. The results indicate that linear response is a reasonable approximation for the solvent's dielectric response beyond the first solvation shell.

S3. RESULTS FOR ALL SOLUTE SIZES INVESTIGATED

In Fig. S3 we show $F_{\mathrm{chg}}^{(\mathrm{var})}$ fitted to F_{chg} obtained from simulation for all solute sizes investigated. For the smallest solutes we see some relatively small discrepancies between the simulation and the theory, but the large degree of charge asymmetry is nevertheless captured. Also shown in Fig. S3 are results for the same solute in different sized simulation boxes, indicating the finite size corrections described in the main text are sufficient to obtain an estimate for the macroscopic charging free energies.

S4. DIELECTRIC RADII

In Fig. S4 we show plot analogous to Fig. 4b in the main article, but for solute sizes $R_0 = 2.70\,\text{Å}$ and $R_0 = 5.50\,\text{Å}$. In both cases we find that R roughly corresponds to the distance of closest approach for the hydrogen atoms of the water molecules.

S5. EQUIPOTENTIAL SURFACES

Figures S5 and S6 show equipotential surfaces arising from dipole and quadrupole contributions, with the multipole expansion respectively performed around the center of charge, and the position of the oxygen atom. Using the center of charge results in an equipotential surface that more closely resembles that of SPC/E water.

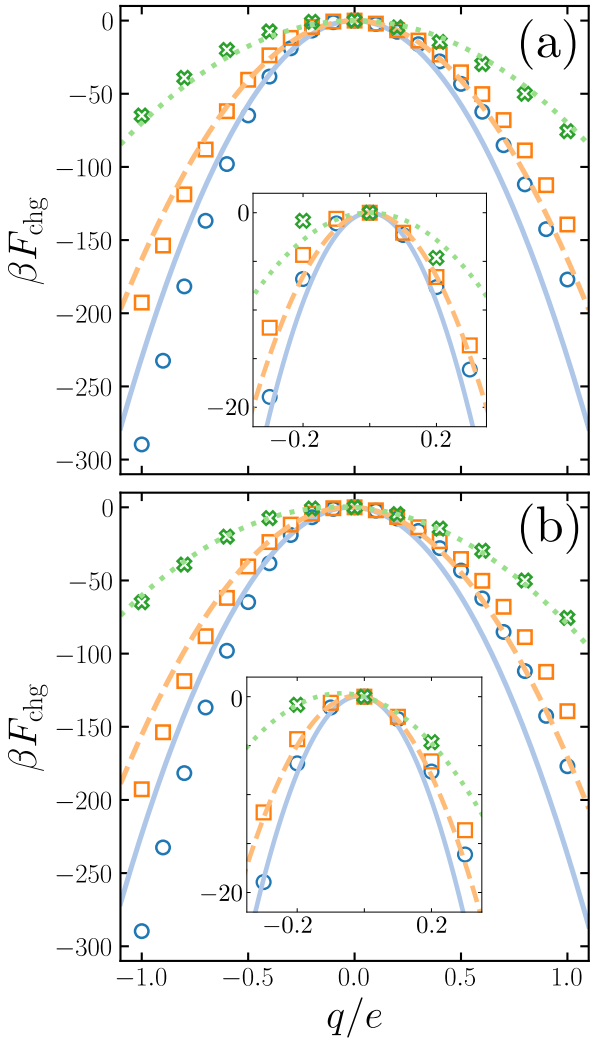

FIG. S1. $F_{\rm chg}$ vs q for different solute sizes R_0: circles, 2.70 Å; squares, 3.17 Å; crosses, 5.50 Å. Symbols show results from simulations. (a) As shown in the main article, $F_{\rm chg}^{\rm (Born)}(q;0)$ (Eq. 5) largely captures the overall scale and size dependence of $F_{\rm chg}$, but it does not describe the asymmetric solvation of anions vs cations. Lines indicate best-fits of $F_{\rm chg}^{\rm (Born)}(q;0)$ to $F_{\rm chg}$. (b) Including a contribution $q\langle V\rangle_0$, $F_{\rm chg}^{\rm (Born)}(q;\langle V\rangle_0)$, only has a small effect, as seen by the similarity to panel (a). In both (a) and (b), the effective Born radii are found to be 1.21 Å (blue circles), 1.69 Å (orange squares) and 3.95 Å (green crosses). Insets: detailed view of the behavior for $-0.3 \le q/e \le 0.3$ where the effect of adding $q\langle V\rangle_0$ is most clear.

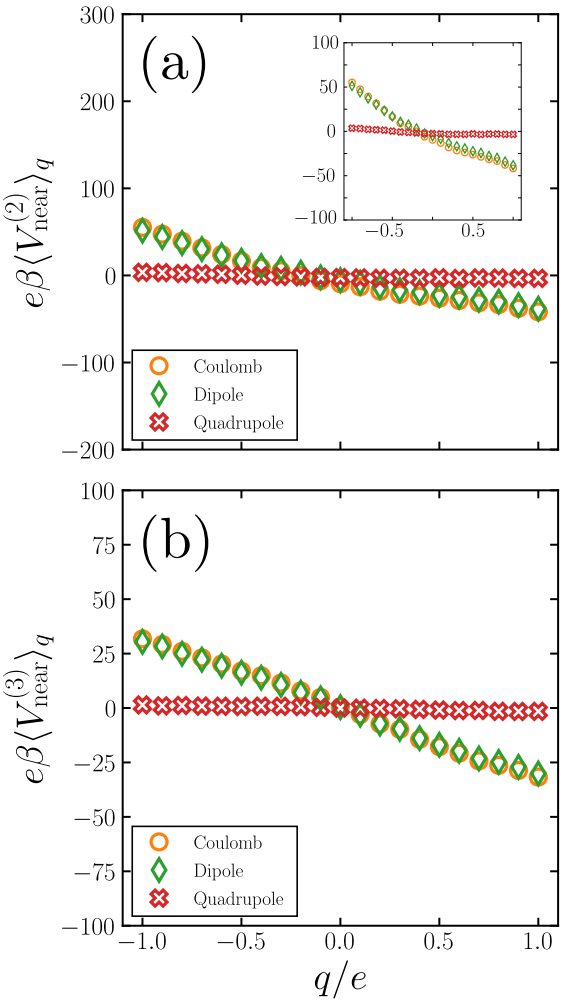

FIG. S2. Contribution to $\langle V\rangle_q$ from more distant solvation shells. The degree on non-linearity is far less pronounced compared to the contributions from the first solvation shell (Fig. 2). (a) $\langle V^{(2)}_{\rm near}\rangle_q$ is the contribution from molecules in the second solvation shell. Inset: same data on a reduced scale, indicating there is still a degree of non-linear response. (b) $\langle V^{(3)}_{\rm near}\rangle_q$ is the contribution from molecules in the third solvation shell.

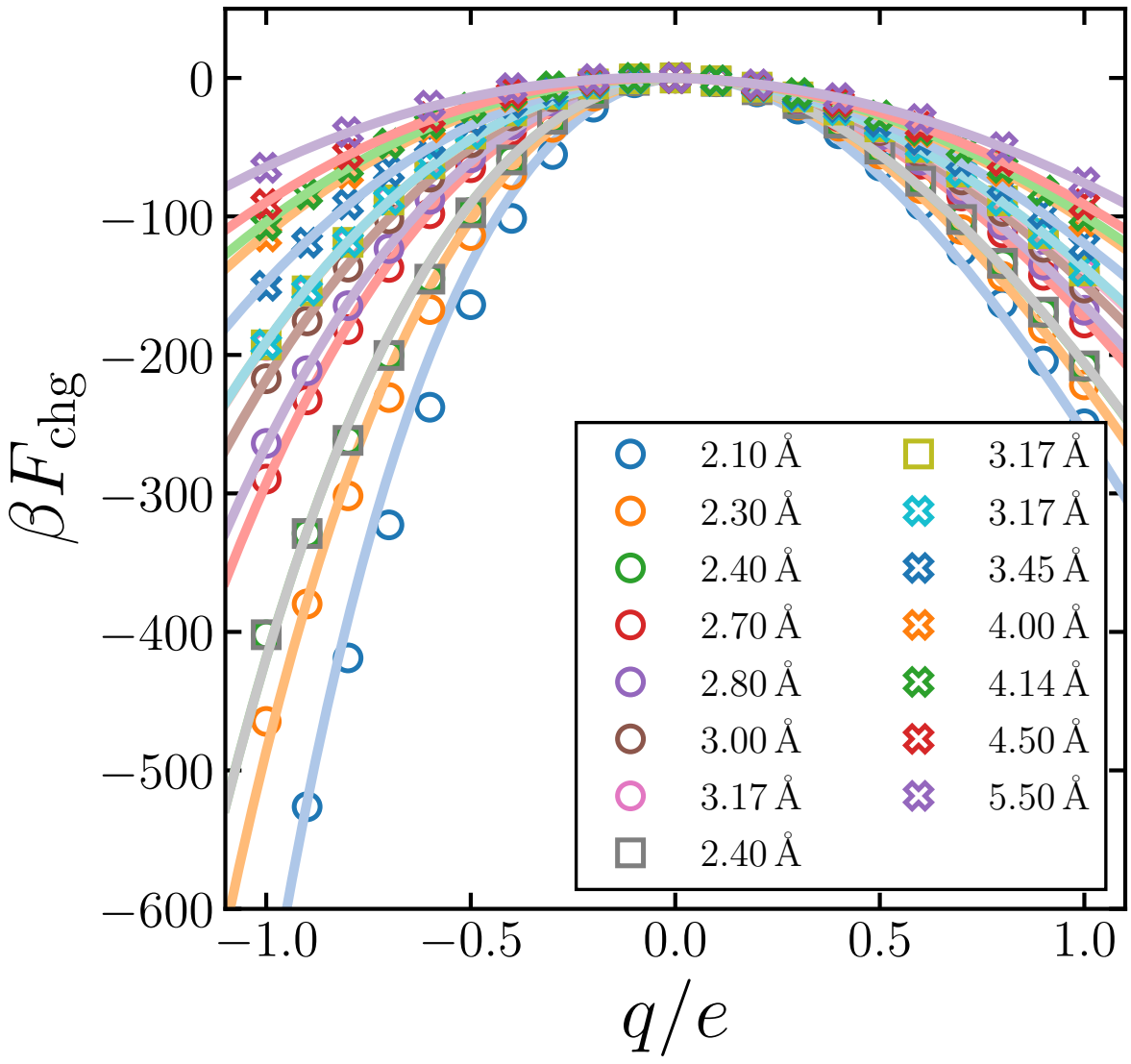

FIG. S3. F_{chg} for all solute sizes studied. Circles, squares and crosses indicate data obtained from simulations with 64, 256 and 512 water molecules, respectively. Results for $R_0 = 2.40\,\text{Å}$ have been obtained with both 64 and 256 water molecules, while for $R_0 = 3.17\,\text{Å}$, F_{chg} has been computed for all three system sizes: these results indicate that the finite size corrections work as expected. Solid lines indicate best fits of $F_{\mathrm{chg}}^{(\mathrm{var})}$ to the simulation data. While some discrepancies are observed for the smallest solutes, the theory does a reasonable job at capturing the charge asymmetry.

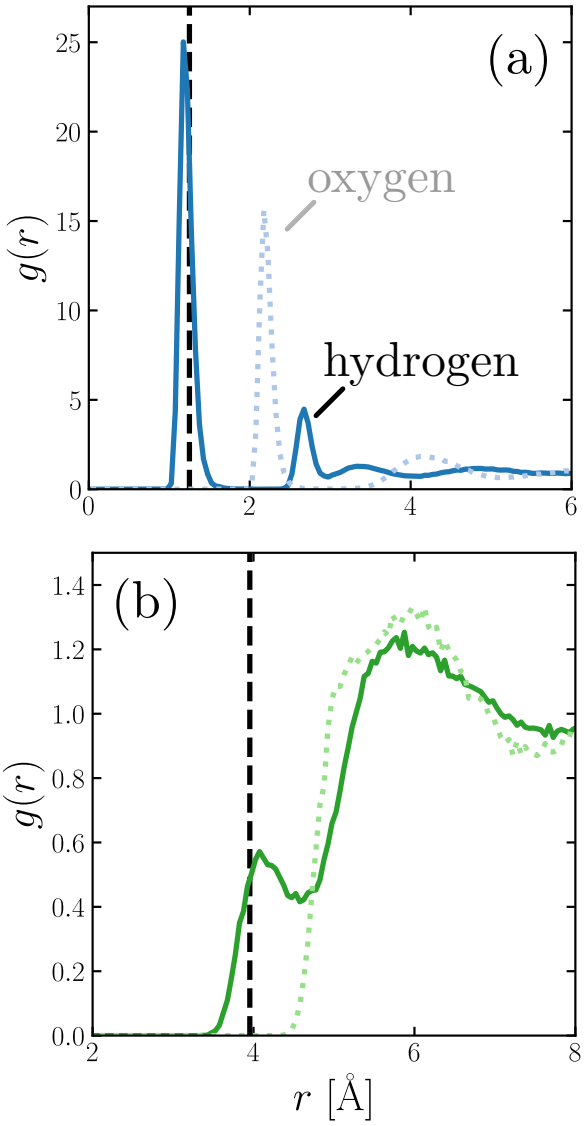

FIG. S4. Solute-solvent radial distribution functions for (a) $R_0 = 2.70\,\text{Å}$ and (b) $R_0 = 5.50\,\text{Å}$. In both cases $q = -e$. Solid and dotted lines show solute-hydrogen $g(r)$ and solute-oxygen $g(r)$, respectively. The vertical dashed line indicates R.

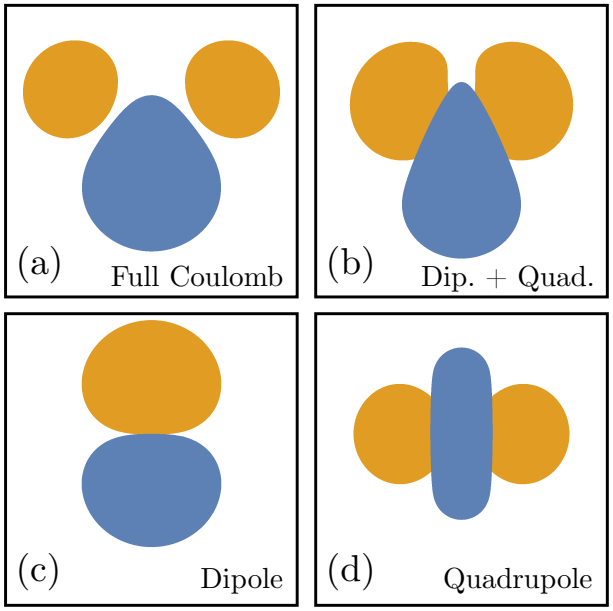

FIG. S5. (a) Equipotential surface of a single water molecule. (b) Equipotential surface resulting from (c) dipole and (d) quadrupole contributions. The center of charge has been used for the multipole expansion.

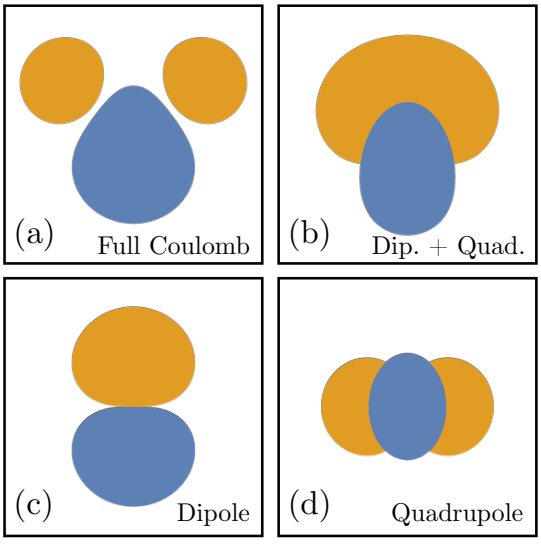

FIG. S6. (a) Equipotential surface of a single water molecule. (b) Equipotential surface resulting from (c) dipole and (d) quadrupole contributions. The position of the oxygen atom has been used for the multipole expansion.